

Design of one-dimensional dielectric and magnetic photonic crystal filters with broad omnidirectional filtering band

HAIXIA QIANG, LIYONG JIANG^{*}, WEI JIA, XIANGYIN LI

Department of Physics, Nanjing University of Science and Technology,
Nanjing 210094, P.R. China

^{*}Corresponding author: jly@mail.njust.edu.cn

A new kind of one-dimensional (1D) photonic crystal (PC) filter is reported in this paper. This kind of a filter is a dimerlike heterostructure constructed by two 1D dielectric and magnetic PCs. Compared with traditional filters based upon 1D pure dielectric PCs, the new one has the advantage of extending the omnidirectional filtering (ODF) band and simplifying the structure due to its large wave impedance contrast between the composites and the reasonable arrangement of the layer thicknesses and the number of periods. To design such a filter, we adopted a combined method by the transmission matrix method and the decimal genetic algorithm, and finally we obtained a high-precision 1D PC filter design which not only shows a very broad relative ODF band of 1.496, but also has a simple structure with less total number of layers and less total thickness. The simplification of structure is conducive to device fabrication. Besides, an example with low dispersive and low dissipative magnetic material for microwave application is also discussed.

Keywords: one-dimensional dielectric and magnetic photonic crystal, filter, transmission matrix method, genetic algorithm.

1. Introduction

Photonic crystals (PCs) have attracted considerable scientific interest during the past decades due to their novel electromagnetic properties and potential applications [1, 2]. In terms of different dimensionalities, PCs are usually classified into three categories: one-dimensional (1D), two-dimensional (2D), and three-dimensional (3D) PCs [3]. The most basic and important character of PCs is the existence of photonic bandgaps (PBGs), in which electromagnetic waves are forbidden, irrespective of propagation direction in space. Despite having no complete PBGs, 1D PCs are still being extensively studied due to their more convenience in fabrication than 2D and 3D PCs and their inherent ability to easily realize omnidirectional total reflection under proper conditions [4, 5].

On the other hand, the easy fabrication and the well-known properties of 1D defective PCs [6–10] made studies on 1D PC filters more attractive and extensive [11–16]. The non-transmission range of a 1D PC filter constructed by a single 1D dielectric PC is sometimes narrow. Some literature revealed that the non-transmission range can be enlarged using heterostructure [17–19]. However, in such structures, the frequencies of defect modes will blue-shift as the incident angle increases. It leads to the fact that light of unwanted frequencies cannot be cut off at some incident angles, which will restrict the applications in some outdoors detections. Filters with the ability of both spatial filtering and large omnidirectional filtering (ODF) band (*i.e.*, omnidirectional reflection band except the frequency of the defect mode) [14, 15] are in urgent need. Recently, a 1D PC filter with dimerlike heterostructure [20, 21] has been proposed. This kind of filter exhibits both narrow-frequency passband and sharp angular pass breadth as well as spatial filtering. However, because the initial proposed model is constructed by quarter-wave pure dielectric layers, in which the omnidirectional total reflection bands of the substructures are not wide enough and overlap each other too much, the ODF band of the filter is still narrow. Alternatively, in our previous work [22], we introduced non-quarter-wave stacks to form a high-precision 1D PC filter. Despite great enhancement of ODF bandwidth, the final heterostructure constructed by three substructures is somehow complicated.

Very recently, WANG *et al.* have demonstrated that there is also a Brewster line for TE polarization in a 1D magnetic PC [23–29], which is similar to that for TM polarization in a 1D dielectric PC. The Brewster line narrows the omnidirectional total reflection band in a 1D pure dielectric or magnetic PC. Since a large permittivity (permeability) benefits the enhancement of TE (TM) band [23, 24, 28, 29], afterwards OUYANG *et al.* [23] and our group [24] demonstrated that arranging high dielectric layers (with large permittivity) and high magnetic ones (with large permeability) periodically to construct a 1D dielectric and magnetic PC can avoid the Brewster lines and effectively enlarge the omnidirectional total reflection band and simplify the structure due to the large wave impedance contrast between the composites. In the present study, we will extend the above idea to design a new filter using 1D dielectric and magnetic PCs to form a dimerlike heterostructure. Furthermore, in agreement with our previous works [22, 24, 30], we will still adopt the transmission matrix method (TMM) in conjunction with the genetic algorithm (GA) [31] to design such structure. The final aim is to obtain a high-precision filter with large ODF band as well as a simple structure.

2. Model and methods

2.1. Transmission matrix in 1D dielectric and magnetic PCs

The 1D PC filter is shown in Fig. 1. It is formed by a typical dimerlike heterostructure described as $(\alpha_1 A, \alpha_2 B)^p (\beta_2 B', \beta_1 A')^p$ which further consists of alternating dielectric

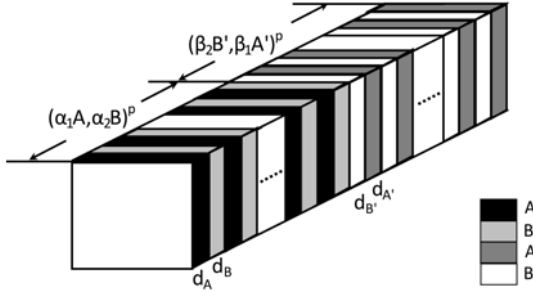


Fig. 1. Schematic of the filter based on the heterostructure $(\alpha_1 A, \alpha_2 B)^p (\beta_2 B', \beta_1 A')^p$.

layer A (A') and magnetic layer B (B') with refractive indices $n_{A(A')}$ and $n_{B(B')}$, where p represents the number of period of each substructure, $\alpha_{1(2)}$ and $\beta_{1(2)}$ represent the thickness ratios of layers. The different designed wavelengths, expressed as λ_L and λ_R , respectively, are applied in the two substructures. The physical thicknesses of layers are $d_A = \alpha_1 \lambda_L / n_A$ and $d_B = \alpha_2 \lambda_L / n_B$ in the left substructure, and $d_{A'} = \beta_1 \lambda_R / n_{A'}$ and $d_{B'} = \beta_2 \lambda_R / n_{B'}$ in the right substructure, respectively. For such a 1D dielectric and magnetic PCs, the transmission can be calculated by the well-known transmission matrix method [32]. The characteristic matrices of layer A (B) and the unit cell AB can be expressed as:

$$\mathbf{M}_{A(B)} = \begin{bmatrix} \cos \beta_{A(B)} & -\frac{i \sin \beta_{A(B)}}{P_{A(B)}} \\ -i P_{A(B)} \sin \beta_{A(B)} & \cos \beta_{A(B)} \end{bmatrix} \quad (1)$$

$$\begin{aligned} \mathbf{M}_{AB} &= \mathbf{M}_A \mathbf{M}_B = \\ &= \begin{bmatrix} \cos \beta_A \cos \beta_B - \frac{p_B \sin \beta_A \sin \beta_B}{p_A} & -i \left(\frac{\cos \beta_A \sin \beta_B}{p_B} + \frac{\sin \beta_A \cos \beta_B}{p_A} \right) \\ -i (p_A \sin \beta_A \cos \beta_B + p_B \cos \beta_A \sin \beta_B) & \cos \beta_A \cos \beta_B - \frac{p_A \sin \beta_A \sin \beta_B}{p_B} \end{bmatrix} \end{aligned} \quad (2)$$

where $\beta_{A(B)} = (\omega/c) n_{A(B)} d_{A(B)} \cos \theta_{A(B)}$, $p_{A(B)} = (\epsilon_{A(B)} / \mu_{A(B)})^{1/2} \cos \theta_{A(B)}$ for TE polarization, and $p_{A(B)} = (\mu_{A(B)} / \epsilon_{A(B)})^{1/2} \cos \theta_{A(B)}$ for TM polarization; ω is the angular frequency of the incident wave, c is the velocity of light in vacuum, and $\theta_{A(B)}$ determined by the Snell's law is the angle between the wave vector and the surface normal vector in layer A (B). Similarly, the characteristic matrix for $A'B'$ is denoted by $\mathbf{M}_{A'B'}$. The transmission matrix for the whole structure can be written as

$$\mathbf{M} = \prod_{i=1}^p \mathbf{M}_{AB}^i \mathbf{M}_{B'A'}^i = \begin{bmatrix} m_{11} & m_{12} \\ m_{21} & m_{22} \end{bmatrix} \quad (3)$$

and the reflectivity and transmissivity can be derived out as

$$R = \left| \frac{(m_{11} + m_{12}p'_0)p_0 - (m_{21} + m_{22}p'_0)}{(m_{11} + m_{12}p'_0)p_0 + (m_{21} + m_{22}p'_0)} \right|^2 \quad (4)$$

$$T = \frac{p'_0}{p_0} \left| \frac{2p_0}{(m_{11} + m_{12}p'_0)p_0 + (m_{21} + m_{22}p'_0)} \right|^2 \quad (5)$$

where $p_0 = (\varepsilon_0/\mu_0)^{1/2} \cos \theta_0$ and $p'_0 = (\varepsilon'_0/\mu'_0)^{1/2} \cos \theta'_0$ for TE polarization, and $p_0 = (\mu_0/\varepsilon_0)^{1/2} \cos \theta_0$ and $p'_0 = (\mu'_0/\varepsilon'_0)^{1/2} \cos \theta'_0$ for TM polarization. θ_0 and θ'_0 represent the incident angle in the ambient media at the left-hand side of the structure and the refractive angle at the right-hand side.

As described in Refs. [20] and [21], during the frequency range of interest, only light with a wavelength $\lambda_0 = (\lambda_L + \lambda_R)/2$ at normal incidence can propagate through the filter with dimerlike quarter-wave heterostructure under the conditions of $n_A = n_{A'}$, $n_B = n_{B'}$, and the filter is sandwiched by the same medium. The transmittance can reach to 100% (perfect transmission). It can be deduced by the transmission matrix method proposed by KOHMOTO *et al.* [33], or Eqs. (1)–(3) and Eq. (5). Therefore, when the layers are no more quarter-wave ones in our new filter, the perfect transmission peak will appear with a wavelength $\lambda_0 = 2(\alpha_1 \lambda_L + \beta_1 \lambda_R) = 2(\alpha_2 \lambda_L + \beta_2 \lambda_R)$ at normal incidence under the similar conditions, namely $Z_A = Z_{A'}$, $Z_B = Z_{B'}$, and the filter is sandwiched by the same medium, where $Z = (\mu/\varepsilon)^{1/2}$ denotes the wave impedance of material. So we only need to optimize the ODF band of the heterostructure, except the location at λ_0 at normal incidence.

2.2. Decimal GA

We use a decimal GA to optimize such structure for broad ODF bandwidth. Compared with the binary GA, the decimal one is faster and more convenient to deal with the decimal variables. In our optimization problem, the GA modifies the design parameters (*i.e.*, the structural parameters, including the thickness ratios and the number of periods) in a way that a better result with larger ODF band would be obtained through steps. The algorithm randomly produces a set of initial designs named the initial population P_0 (containing N_c initial chromosomes). Each chromosome consists of several gene segments. There are three gene segments for the heterostructure. Each segment represents the value of a decision variable, *i.e.* one of α_1 (β_1), α_2 (β_2), and p . Due to the relationship between α_1 (α_2) and β_1 (β_2), *i.e.* $\lambda_0 = 2(\alpha_1 \lambda_L + \beta_1 \lambda_R) =$

$= 2(\alpha_2\lambda_L + \beta_2\lambda_R)$, the number of the variables is reduced to three. Then, without being encoded in the GA, all chromosomes in the initial population are just evaluated according to an objective function, which measures the fitness value of a solution to a given problem as well as can represent the quantity optimized by the GA. In particular, our goal is to increase reflectivity to a maximum for all frequencies ω_{r_i} ($i = 1, 2, \dots, 2001$; $\omega_{r_i} = (i - 1)\omega_0/1000$, where $\omega_0 = 2\pi c/\lambda_0$ denotes the preassigned filtering frequency) except ω_0 with any incident angle θ_j ($j = 1, 2, \dots, 90$, $\theta_j = (j - 1)^\circ$) and both polarizations. Accordingly, the objective function can be expressed by

$$F_{\text{ODF}} = \frac{\omega_0 \sum_{i=1} B(\omega_{r_i})}{1000} \quad (6)$$

where

$$B(\omega_{r_i}) = \begin{cases} 1 & R(\omega_{r_i}, \theta_j) \geq R_{\text{ref}} \\ 0 & R(\omega_{r_i}, \theta_j) < R_{\text{ref}} \end{cases}, \quad (\text{for } \forall \theta_j \text{ and polarization}) \quad (7)$$

R_{ref} is the referenced reflectance. Here, we set it as 99.5%. When $R(\omega_{r_i}, \theta_j) \geq R_{\text{ref}}$ (for any θ_j and polarization), the incident wave can be thought of as the total reflection.

Then the GA works by iteratively using three genetic operators that are selection, crossover and mutation to evolve the population. The working process of the three operations is given as follows, and the detailed information is available in Ref. [31]. The selection operator (also known as roulette-wheel selection) chooses two chromosomes randomly from the original population P_0 and keeps down the better one with higher fitness value to form a new population. This process is repeated until the new population P_s contains N_c chromosomes. Then the crossover operator randomly chooses a pair of parent chromosomes from P_s . The two parent chromosomes are mated with a given probability p_c to generate two offspring. With the crossover process repeated, another new population P_{sc} is created. After crossover, mutation operator is applied to prevent premature convergence. Mutation produces spontaneous random changes in various chromosomes. It takes place with a predetermined mutation probability p_m . After mutation, the chromosomes of the new population P_{scm} are reevaluated, and the process begins anew with selection.

The algorithm is terminated when either a design goal is reached, or no process is observed in the population for several generations, which is usually represented by a maximum generation N_G . Finally, the best chromosome will provide the optimum solution. Note that p_c and p_m play a critical role in the GA. In particular, we choose $p_c = 0.9$ and $p_m = 0.005$ in this paper according to many GA designers recommend. Moreover, considering both calculation precision and velocity, we set $N_c = 200$ and $N_G = 40$ for all calculations.

3. Calculation results and discussions

3.1. Ideal case for arbitrary wavelength region

In this section, we will give some calculation results for the filter model $(\alpha_1 A, \alpha_2 B)^p (\beta_2 B', \beta_1 A')^p$ considering $\varepsilon_{A(A')} = 5.29$, $\mu_{A(A')} = 1$, $\varepsilon_{B(B')} = 1.5$, $\mu_{B(B')} = 4.17$, $\varepsilon_0 = 1$, $\mu_0 = 1$, $\varepsilon'_0 = 1$ and $\mu'_0 = 1$ [23]. First of all, since our model is unknown prior to optimization, the searching areas of the thickness ratios and the number of periods have to be determined. From a practical point of view, any substantial increase in the layer thickness is undesirable due to the possible strain arising in the layer itself or at the interface between the layer and the substrate, so both α_i ($i = 1, 2$) and β_i ($i = 1, 2$) are limited in the range of 0–0.300. Moreover, the whole system should be compact and simple, so the searching area of p is reasonably limited in the range of 1–16 taking the practical applicability into account.

The GA optimization for the heterostructure was executed by a personal computer with the processor Pentium 4 Intel 3.0 GHz and 2.0 Gigabyte memory. The total optimization costs 35 hours and 12 minutes and the searching process for the best fitness in each generation is shown in Fig. 2. It is found that the process reaches convergence at the 21-th generation and an optimal design described as $(0.191A, 0.201B)^{14} (0.2878B', 0.2955A')^{14}$ is achieved. The relative ODF bandwidth for the structure reaches 1.496 and the corresponding reflection spectra are shown in Fig. 3c. In particular, for comparison purpose, Figs. 3a and 3b give the reflection spectra for the substructures $(0.191A, 0.201B)^{14}$ and $(0.2878B', 0.2955A')^{14}$, while Figs. 3d–3f present the reflection spectra for the quarter-wave dielectric and magnetic structures $(0.25A, 0.25B)^{14}$, $(0.25B', 0.25A')^{14}$ and $(0.25A, 0.25B)^{14} (0.25B', 0.25A')^{14}$. It is clearly found from Figs. 3d and 3e that the omnidirectional total reflection bands of the quarter-wave substructures overlap each other too much. Consequently, it gives rise to a narrow ODF band (as shown in Fig. 3f) when the substructures are stacked symmetrically to form a quarter-wave dimerlike heterostructure. In our optimal design, the omnidirectional total reflection bands of the substructures are adjacent to each other as shown in Figs. 3a and 3b. Moreover, there is much less superposition of the bands. Thus, the ODF band can be extended sufficiently in the corresponding heterostructure.

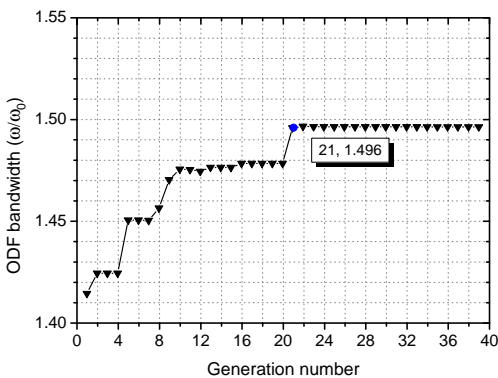


Fig. 2. Statistic information on the searching process.

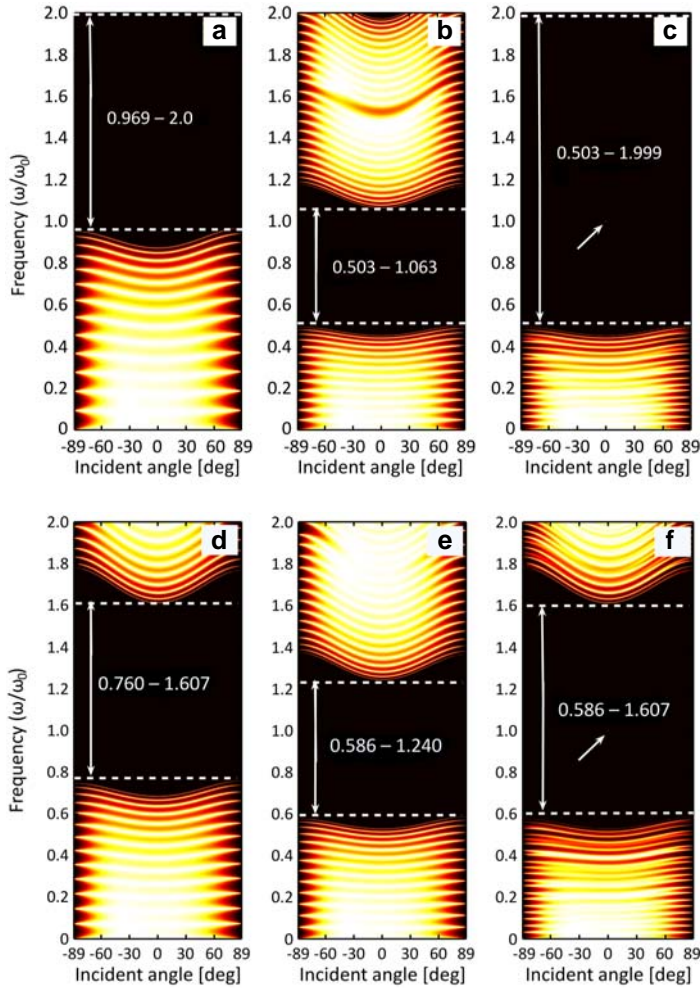


Fig. 3. Transmission spectra of the structures: the optimal substructure $(0.191A, 0.201B)^{14}$ (a); the optimal substructure $(0.2878B', 0.2955A')^{14}$ (b); the optimal heterostructure $(0.191A, 0.201B)^{14} - (0.2878B', 0.2955A')^{14}$ (c); the quarter-wave dielectric and magnetic substructure $(0.25A, 0.25B)^{14}$ (d); the quarter-wave dielectric and magnetic substructure $(0.25B', 0.25A')^{14}$ (e); the quarter-wave dielectric and magnetic heterostructure $(0.25A, 0.25B)^{14}(0.25B', 0.25A')^{14}$ (f), where the incident angles from -89° to 0° represent the case of TM polarization, while 0° to 89° for the case of TE, the area between the two dashed lines represents the omnidirectional total reflection band or ODF band, and the arrow indicates the position of the filtering frequency.

The results indicate that optimizing the thickness using the GA can effectively enlarge the ODF band of the filter.

To make a detailed comparison with the filters reported in previous works [21, 22], we prepared a table to give the information about the performance and structure complexity in each design as indicated in Tab. 1. Note that S1 in Tab. 1 denotes the structure in Ref. [21], while S2 for the structure in our previous work [22]. S3 and

T a b l e 1. Some performance parameters for different heterostructures. (To be continued on next page.)

Structure	Materials	Thickness ratios
S1: $(\alpha_1 A, \alpha_2 B)^{14} (\beta_2 B', \beta_1 A')^{14}$	Dielectric	0.25, 0.25, 0.25, 0.25
S2: $\alpha \left[(A, B)^8 (B, A)^8 \right] \beta (A, B)^8$ $\beta (A, B)^8 \gamma \left[(A, B)^8 (B, A)^8 \right]$	Dielectric	0.1545, 0.25, 0.3455
S3: $(\alpha_1 A, \alpha_2 B)^{14} (\beta_2 B', \beta_1 A')^{14}$	Dielectric and magnetic	0.25, 0.25 0.25, 0.25
S4: $(\alpha_1 A, \alpha_2 B)^{14} (\beta_2 B', \beta_1 A')^{14}$	Dielectric and magnetic	0.191, 0.201, 0.2878, 0.2955

S4 denote the structures in Figs. 3f and 3c, respectively. It can be derived from Tab. 1 that our optimal design owns the widest ODF band whereas the total number of layers and the total thickness are the least, which makes our design applicable in optical filters, optical switches and other optical devices. The above results indicate that the introduction of magnetic materials and the proper arrangement of structural parameters can indeed enlarge the ODF band and simplify the whole structure, and GA is an effective optimizing tool in designing 1D PC filters with wide ODF band.

Another point to be discussed is the filtering characteristic of the optimal design. As shown in Fig. 4a, the structure provides a very narrow-frequency passband. Besides, the switching behavior of the filter is shown in Fig. 4b. It is well-known that the blueshift happens to both PBGs and defect modes as the incident angle changes from normal to an oblique direction [15, 16]. However, in our system, when the incident beam in TE and TM polarization is tilted only a negligibly small angle,

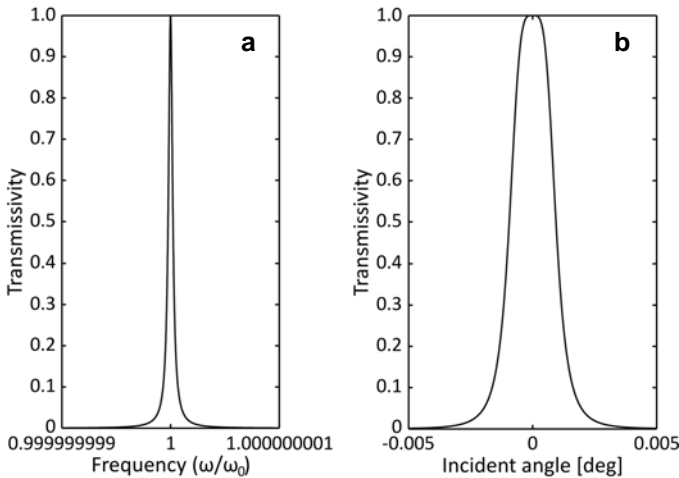


Fig. 4. Transmission spectra of the optimal heterostructure $(0.191A, 0.201B)^{14} (0.2878B', 0.2955A')^{14}$ at frequency from 0.999999999 to 1.000000001 at normal incidence (a), and at frequency ω_0 at incident angles from -0.005° to 0.005° , where incident angles from -0.005° to 0° represent the case of TM polarization, while 0° to 0.005° for the case of TE (b).

Tab. 1. Continued.

ODF band ω/ω_0	ODF bandwidth ω/ω_0	Total number of layers	Total thickness λ_0
0.828–1.421	0.593	56	6.2945
0.600–1.999	1.399	96	9.9706
0.586–1.607	1.021	56	5.8435
0.503–1.999	1.496	56	5.8435

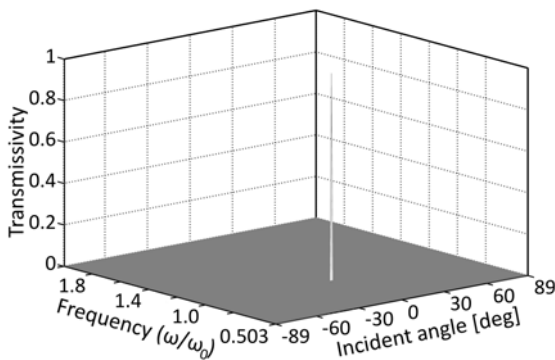


Fig. 5. Transmission spectra of the optimal heterostructure $(0.191A, 0.201B)^{14}(0.2878B', 0.2955A')^{14}$, where incident angles from -89° to 0° represent the case of TM polarization, while 0° to 89° for the case of TE.

e.g., from -0.005° to 0.005° , a switching behavior of the defect mode takes place: the perfect transmission peak clearly vanishes. (The transmissivity sharply approaches null.) Figure 5 shows the transmission spectra of the filter as functions of the incident angle and frequency. It is distinctly observed that only light within a very narrow frequency passband and a sharp breadth of incident angle is allowed to be perfectly transmitted in the ODF band ranging from $0.503\omega_0$ to $1.999\omega_0$.

3.2. An example for microwave region

The optimal results in Section 3.1 are based on ideal materials. However, some difficulties arise in practice: first, nearly all materials are dispersive; second, materials, especially magnetic materials, are usually dissipative at high frequency region. These adverse factors will greatly affect the PBG greatly and make the ODF band narrow. Hence, magnetic materials with stable electromagnetic parameters (permittivity and permeability) are needed for practical application. At the beginning of 1990s, a new kind of magnetic materials, termed organometallic magnets, is proposed [34]. Such materials provide stable dependence of electromagnetic parameters on frequencies from 100–17000 MHz [35, 36]. Moreover, the absorption which can be controlled or

Table 2. Electromagnetic parameters $\varepsilon_B = \varepsilon'_B + i\varepsilon''_B$ and $\mu_B = \mu'_B + i\mu''_B$ of ferrocene type polymeric magnet at different frequencies [36].

Frequency [GHz]	0.1	0.3	0.5	0.8	1.0	1.3	1.5	1.8
μ'_B	1.2	1.2	1.3	1.3	1.4	1.5	1.6	2.0
$\mu''_B (\times 10^{-3})$	1	1	1	1	1	1	1	2
ε'_B	4.5	4.6	4.6	4.6	4.6	4.6	4.6	4.6
$\varepsilon''_B (\times 10^{-3})$	1	1	1	1	1	1	1	1

reduced by the preparation process or the dosage of materials [36] is extremely low compared with inorganic magnets. In this section, we will optimize a filter with organometallic magnetic materials for microwave application using GA, and the effect of dissipation on filtering characteristic will also be investigated.

The transmissivity at the filtering frequency is very sensitive to the dissipation. Generally, lower dissipation corresponds to better designs. So a dispersive model without absorption is considered at first. The magnetic material used here is ferrocene type polymeric magnet [36]. The electromagnetic parameters $\varepsilon_B = \varepsilon'_B + i\varepsilon''_B$ and $\mu_B = \mu'_B + i\mu''_B$ obtained from the experiment in Ref. [36] are shown in Tab. 2. The electromagnetic parameters between every two sampling points in Tab. 2 are evaluated by linear interpolation in calculation process. Note that the permeability is lower than the permittivity in such material, which causes a low wave impedance contrast. But the example can still validate our optimizing method. The other material is gallium arsenide with invariable parameters as $\varepsilon_A = 12.96$ and $\mu_A = 1$. It should be noted that the condition $\lambda_0 = 2(\alpha_1\lambda_L + \beta_1\lambda_R) = 2(\alpha_2\lambda_L + \beta_2\lambda_R)$ for ensuring perfect transmission at the predetermined filtering frequency is only required at this frequency, so the thicknesses of the magnetic films should be determined as $d_B = \alpha_2\lambda_L/n_{B, \text{filtering}}$, and $d_{B'} = \beta_2\lambda_R/n_{B', \text{filtering}}$, where ($i = B, B'$) represents the refractive index at the filtering frequency. Thus, a unique and optimal thickness combination of our design will be obtained after optimization.

The optimization on the structure $(\alpha_1A, \alpha_2B)^p(\beta_2B', \beta_1A')^p$ was executed with $\varepsilon'' = 0$ and $\mu'' = 0$. The optimal structure is $(0.199A, 0.28B)^{15}(0.2893A', 0.2269B')^{15}$ with 60 layers and total thickness of 0.4244 m ($5.0930\lambda_0$). The corresponding transmission spectra are shown in Fig. 6c. The ODF band of the heterostructure is 0.657 GHz ($0.73\omega_0$) in the range of 0.747 to 1.404 GHz. For comparison purpose, we have also calculated the transmission spectra of the quarter-wave structure $(0.25A, 0.25B)^{15}(0.25A', 0.25B')^{15}$. The ODF band is 0.6 GHz ($0.67\omega_0$) in the range of 0.773 to 1.373 GHz. These results indicate that the optimal design provides wider ODF band and less total thickness than those of S1 in Tab. 1 and the heterostructure $(0.25A, 0.25B)^{15}(0.25A', 0.25B')^{15}$. Moreover, the increment will be enhanced further by using other organometallic magnetic material with larger wave impedance contrast. Besides, as shown in Figs. 7c and 7f, the optimal design also owns very narrow passband and sharp angular pass breadth at the filtering frequency 0.9 GHz.

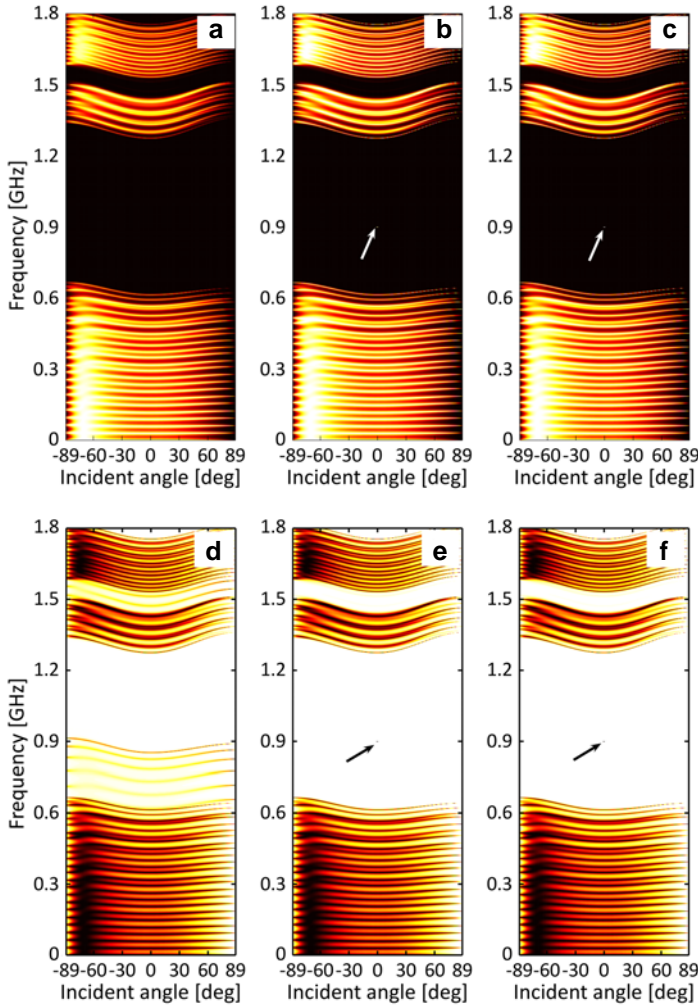


Fig. 6. Transmission (a–c) and reflection (d–f) spectra of the optimal heterostructure $(0.199A, 0.28B)^{15}(0.2893A', 0.2269B')^{15}$ with $\epsilon'' = 0.001$ and $\mu'' = 0.001$ (a, d), $\epsilon'' = 0.0000001$ and $\mu'' = 0.0000001$ (b, e), $\epsilon'' = 0$ and $\mu'' = 0$ (c, f), where the black region in (a–c) represents low transmission region with transmissivity less than 0.005, while the white region in (d–f) represents high reflection region with reflectivity larger than 0.995.

Based on the above optimal design, we consider the magnetic material with $\epsilon'' \neq 0$ and $\mu'' \neq 0$. For simplicity, ϵ'' and μ'' are not dispersive here. Figures 6 and 7 show the transmission and reflection spectra of the heterostructure $(0.199A, 0.28B)^{15}(0.2893A', 0.2269B')^{15}$ with different ϵ'' and μ'' . It is found from Fig. 6 that the ODF band in transmission spectra changes slightly, while the ODF band in the reflection spectra reduces obviously as ϵ'' and μ'' increase. The summation

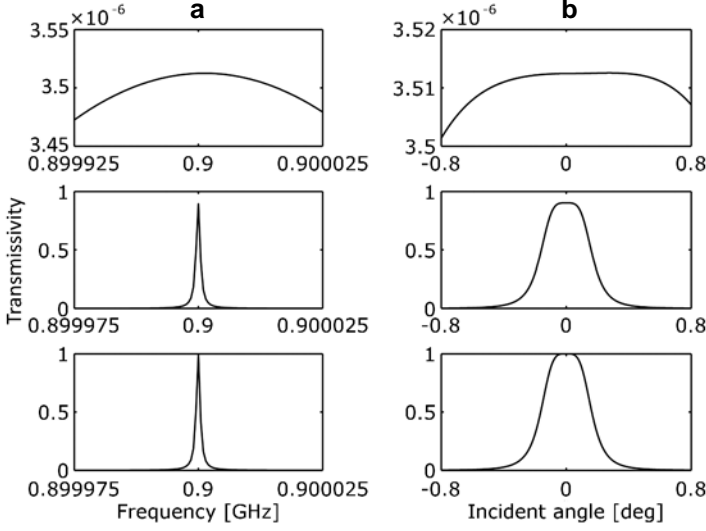


Fig. 7. Transmission spectra of the optimal heterostructure $(0.199A, 0.28B)^{15}(0.2893A', 0.2269B')^{15}$ at frequency from 0.899975 to 0.900025 at normal incidence (a), and at frequency ω_0 at incident angles from -0.8° to 0.8° , where incident angles from -0.8° to 0° represent the case of TM polarization, while 0° to 0.8° for the case of TE (b).

of the transmissivity and the reflectivity at any frequency is lower than 1 due to material absorption. These results indicate that we could replace Eq. (7) by

$$B(\omega_{r_i}) = \begin{cases} 1 & T(\omega_{r_i}, \theta_j) \leq T_{\text{ref}} \\ 0 & T(\omega_{r_i}, \theta_j) > T_{\text{ref}} \end{cases}, \quad (\text{for } \forall \theta_j \text{ and polarization}) \quad (8)$$

if the absorption is considered in optimizing process, where T_{ref} is the referenced transmittance set as 0.5%, and when $T(\omega_{r_i}, \theta_j) \leq T_{\text{ref}}$ (for any θ_j and polarization), the incident wave can be thought of as non-transmission. Thus, the optimizing method can be still successfully used to obtain wider ODF band of dissipative 1D PC. Besides, it is clearly found from Fig. 7 that the filtering peak at 0.9 GHz is completely suppressed when $\varepsilon'' = 0.001$ and $\mu'' = 0.001$, while it decreases only a little when $\varepsilon'' = 0.0000001$ and $\mu'' = 0.0000001$. Both the frequency pass band and the angle pass breadth increase as ε'' and μ'' increase, which is undesirable for switching behavior of filters. These results indicate that the performance of the optimal filter is very sensitive to the dissipation, and such performance degeneration may be unavoidable before magnetic materials with both extremely low ε'' and μ'' at high frequency region is available in practice. Therefore we should do further work on preparation of magnetic materials with extremely low absorption.

4. Conclusions

In summary, a high-precision filter with broad ODF band has been designed using the 1D dielectric and magnetic PCs. This filter, described as $(0.191A, 0.201B)^{14} - (0.2878B', 0.2955A')^{14}$, shows a relative ODF range from 0.503 to 1.999 with a very narrow-frequency and sharply angular transmission window at normal incidence. Compared with many designs in previous works, such filter has the advantage of both ODF bandwidth and structure complexity. This outstanding performance is mainly attributed to the proper arrangement of the structural parameters, and the large wave impedance contrast between the composites which is beneficial to remove the influence of Brewster lines for TM and TE polarizations. Besides, an example with low dispersive and low dissipative magnetic materials for microwave application is also discussed. The optimal designs in this work have some potential applications in high-quality optical filters, optical switches, mobile telephone antennae and other optical devices.

Acknowledgements – This work was supported by the research fund of Nanjing University of Science and Technology (NJUST) (No. 2010ZYTS059, No. AE88030) and the Natural Science Foundation of Jiangsu Province (No. BK2010483).

References

- [1] YABLONOVITCH E., *Inhibited spontaneous emission in solid-state physics and electronics*, Physical Review Letters **58**(20), 1987, pp. 2059–2062.
- [2] JOHN S., *Strong localization of photons in certain disordered dielectric superlattices*, Physical Review Letters **58**(23), 1987, pp. 2486–2489.
- [3] SAKODA K., *Optical Properties of Photonic Crystals*, 2nd Edition, Springer-Verlag, Berlin Heidelberg, 2005.
- [4] WINN J.N., FINK Y., FAN S.H., JOANNOPOULOS J.D., *Omnidirectional reflection from a one-dimensional photonic crystal*, Optics Letters **23**(20), 1998, pp. 1573–1575.
- [5] FINK Y., WINN J.N., FAN S.H., CHEN C.H., MICHEL J., JOANNOPOULOS J.D., THOMAS E.L., *A dielectric omnidirectional reflector*, Science **282**(5394), 1998, pp. 1679–1682.
- [6] YABLONOVITCH E., GMITTER T.J., MEADE R.D., RAPPE A.M., BROMMER K.D., JOANNOPOULOS J.D., *Donor and acceptor modes in photonic band structure*, Physical Review Letters **67**(24), 1991, pp. 3380–3383.
- [7] FORESI J.S., VILLENEUVE P.R., FERRERA J., THOEN E.R., STEINMEYER G., FAN S., JOANNOPOULOS J.D., KIMERLING L.C., SMITH H.I., IPPEN E.P., *Photonic-bandgap microcavities in optical waveguides*, Nature **390**(6656), 1997, pp. 143–145.
- [8] NODA S., CHUTINAN A., IMADA M., *Trapping and emission of photons by a single defect in a photonic bandgap structure*, Nature **407**(6804), 2000, pp. 608–610.
- [9] SHI B., JIANG Z.M., WANG X., *Defective photonic crystals with greatly enhanced second-harmonic generation*, Optics Letters **26**(15), 2001, pp. 1194–1196.
- [10] STEINBERG B.Z., BOAG A., LISITSIN R., *Sensitivity analysis of narrowband photonic crystal filters and waveguides to structure variations and inaccuracy*, Journal of the Optical Society of America A **20**(1), 2003, pp. 138–146.

- [11] FENG QIAO, CHUN ZHANG, JUN WAN, JIAN ZI, *Photonic quantum-well structures: Multiple channeled filtering phenomena*, Applied Physics Letters **77**(23), 2000, pp. 3698–3700.
- [12] HA Y.-K., YANG Y.-C., KIM J.-E., PARK H.Y., KEE C.-S., LIM H., LEE J.-C., *Tunable omnidirectional reflection bands and defect modes of a one-dimensional photonic band gap structure with liquid crystals*, Applied Physics Letters **79**(1), 2001, pp. 15–17.
- [13] PENG R.W., HUANG X.Q., QIU F., WANG M., HU A., JIANG S.S., MAZZER M., *Symmetry-induced perfect transmission of light waves in quasiperiodic dielectric multilayers*, Applied Physics Letters **80**(17), 2002, pp. 3063–3065.
- [14] LIANG G.Q., HAN P., WANG H.Z., *Narrow frequency and sharp angular defect mode in one-dimensional photonic crystals from a photonic heterostructure*, Optics Letters **29**(2), 2004, pp. 192–194.
- [15] SHAOJI JIANG, YAN LIU, GUANQUAN LIANG, HEZHOU WANG, , *Design and fabrication of narrow-frequency sharp angular filters*, Applied Optics **44**(30), 2005, pp. 6353–6356.
- [16] KUN-YUAN XU, XIGUANG ZHENG, CAI-LIAN LI, WEI-LONG SHE, *Design of omnidirectional and multiple channeled filters using one-dimensional photonic crystals containing a defect layer with a negative refractive index*, Physical Review E **71**(6), 2005, p. 066604.
- [17] WANG LI, WANG ZHAN-SHAN, SANG TIAN, WU YONG-GANG, CHEN LING-YAN, LIU HUA-SONG, JI YI-QIN, *Broadening of non-transmission band of ultra-narrow band-pass filters using heterostructures*, Chinese Physics Letters **25**(6), 2008, pp. 2030–2032.
- [18] ZHANSHAN WANG, LI WANG, YONGGANG WU, LINGYAN CHEN, XIAOSHUANG CHEN, WEI LU, *Multiple channeled phenomena in heterostructures with defects mode*, Applied Physics Letters **84**(10), 2004, pp. 1629–1631.
- [19] LI WANG, ZHANSHAN WANG, YONGGANG WU, LINGYAN CHEN, SHAOWEI WANG, XIAOSHUANG CHEN, WEI LU, *Enlargement of the non transmission frequency range of multiple-channeled filters by the use of heterostructures*, Journal of Applied Physics **95**(2), 2004, pp. 424–426.
- [20] LU Y., PENG R.W., WANG Z., TANG Z.H., HUANG X.Q., WANG M., QIU Y., HU A., JIANG S.S., FENG D., *Resonant transmission of light waves in dielectric heterostructures*, Journal of Applied Physics **97**(12), 2005, p. 123106.
- [21] LU Y.H., HUANG M.D., PARK S.Y., KIM P. J., NAHM T.-U., LEE Y.P., RHEE J.Y., *Controllable switching behavior of defect modes in one-dimensional heterostructure photonic crystals*, Journal of Applied Physics **101**(3), 2007, p. 036110.
- [22] WEI JIA, LIYONG JIANG, GAIGE ZHENG, XIANGYIN LI, HAIPENG LI, *Broad omnidirectional high-precision filters design using genetic algorithm*, Optics and Laser Technology **42**(2), 2010, pp. 382–386.
- [23] OUYANG Z.B., MAO D.P., LIU C.P., WANG J.C., *Photonic structures based on dielectric and magnetic one dimensional photonic crystals for wide omnidirectional total reflection*, Journal of the Optical Society of America B **25**(3), 2008, pp. 297–301.
- [24] HAIXIA QIANG, LIYONG JIANG, XIANGYIN LI, *Design of broad omnidirectional total reflectors based on one-dimensional dielectric and magnetic photonic crystals*, Optics and Laser Technology **42**(1), 2010, pp. 105–109.
- [25] SIGALAS M.M., SOUKOULIS C.M., BISWAS R., HO K.M., *Effect of the magnetic permeability on photonic band gaps*, Physical Review B **56**(3), 1997, pp. 959–962.
- [26] LYUBCHANSKII I.L., DADOENKOVA N.N., LYUBCHANSKII M.I., SHAPOVALOV E.A., RASING T., *Magnetic photonic crystals*, Journal of Physics D: Applied Physics **36**(18), 2003, pp. R277–R287.
- [27] LINDEN S., DECKER M., WEGENER M., *Model system for a one-dimensional magnetic photonic crystal*, Physical Review Letters **97**(8), 2006, p. 083902.
- [28] CHUL-SIK KEE, JAE-EUN KIM, HAE YONG PARK, *Omnidirectional reflection bands of one-dimensional magnetic photonic crystals*, Journal of Optics A: Pure and Applied Optics **6**(12), 2004, pp. 1086–1088.
- [29] WANG Z., LIU D., *A few points on omnidirectional band gaps in one-dimensional photonic crystals*, Applied Physics B: Lasers and Optics **86**(3), 2007, pp. 473–476.
- [30] LIYONG JIANG, GAIGE ZHENG, LINXING SHI, JUN YUAN, XIANGYIN LI, *Broad omnidirectional reflectors design using genetic algorithm*, Optics Communications **281**(19), 2008, 4882–4888.

- [31] BOOZARJOMEHRY R.B., MASOORI M., *Which method is better for the kinetic modeling: Decimal encoded or Binary Genetic Algorithm?*, Chemical Engineering Journal **130**(1), 2007, pp. 29–37.
- [32] BORN M., WOLF E., *Principles of Optics*, 6th Edition, Pergamon Press, Oxford, 1980.
- [33] KOHMOTO M., SUTHERLAND B., IGUCHI K., *Localization of optics: Quasiperiodic media*, Physical Review Letters **58**(23), 1987, pp. 2436–2438.
- [34] MILLER J.S., EPSTEIN A.J., SILVER J., *Organometallic ferromagnets*, Philosophical Transactions of the Royal Society of London A **330**(1610), 1990, pp. 205–215.
- [35] ZHANRU LIN, *Organometallic polymers with ferromagnetic properties*, Advanced Materials **11**(13), 1999, pp. 1153–1154.
- [36] AN Q.Z., PENG H.Q., LIN Y., LIN Z.R., *Studies on the dielectric and magnetic properties of ferrocene type polymeric magnetic modified by acrylic acid*, Journal of Sichuan Normal University (Natural Science) **25**(5), 2002, pp. 500–502 (in Chinese).

*Received April 23, 2010
in revised form September 13, 2010*